RF-MEMS Phased Array Antenna on Low-Loss LTCC Substrate for Ka-Band Data Link

William Gautier°[1], Volker Ziegler[#], Armin Stehle°, Bernhard Schoenlinner[#], Ulrich Prechtel[#], Wolfgang Menzel[*]

°EADS Deutschland GmbH, Defence Electronics, Woerthstr. 85, D-89077 Ulm, Germany

[1]william.gautier@eads.com

[#]EADS Deutschland GmbH, Innovation Works, Willy-Messerschmitt-Str., D-85521 Ottobrunn, Germany

[*]University of Ulm, Institute of Microwave Techniques, Albert-Einstein-Allee 41, D-89069 Ulm, Germany

***Abstract*— In this paper, an electrically steerable antenna for communication at Ka-band is demonstrated. The antenna itself is a microstrip antenna array made out of low-loss LTCC (Low Temperature Co-fired Ceramics) DuPont 943 substrate. The antenna is made electrically steerable in the H–plane of the aperture by means of RF-MEMS phase shifters. The phase shifters are 3-bit phase shifters processed in the EADS Innovation Works RF-MEMS technology. They are integrated in a hybrid fashion onto the ceramic substrate of the antenna. The paper describes the different development steps of the complete phased array antenna, including the design of the antenna array, and the integration of the phase shifters. Finally, the design and the realisation of the phased antenna demonstrator are assessed and validated by satisfactory measurement results.**

I. Introduction

Since the advent of satellite communication in the late 60's, two kinds of antenna have been widely implemented in satellite transceivers: parabolic dishes on-board of large satellites, and omni-directional antennas in small satellites. Thanks to their directional pattern, parabolic dishes enable high transmission data rates, and they allow for a reduced transmit or receive power that can be fully dedicated to, or received from a given targeted area. However, because they are too large, parabolic dishes cannot be used in small satellites having limited payloads. Also, in most cases, these satellites are constraint to operate with omni-directional antennas assuming modest performance. Furthermore, due to their sensitivity to inertia, the beam scanning mandatory for a majority of modern satellite communication systems is not possible with a mechanically steerable antenna on-board of micro-satellites. To overcome this situation, electrically steerable antennas have been recently considered for implementation in small satellites [1], [2]. On the other hand, and besides the increased performance that phased antennas enable for communication links, they offer un-precedent opportunities for micro- and nano-satellites in the field of imaging and earth observation [3], [4].

The antenna demonstrated in this paper is a phased antenna array designed for uplink satellite communication at 35 GHz. The antenna is electrically steerable in the H-plane of the aperture, and it assumes a fixed broadside pattern in the E-plane. In order to facilitate the integration of the antenna in the complete front-end, a ceramic dielectric has been preferred to an organic soft substrate for the realisation of the antenna. The antenna is made out of a low-loss 6-layer LTCC DuPont 943 substrate (ε_r=7.4, tanδ=0.0015). In a further integration step, these layers could be the top layers of a 3D integrated millimetre wave LTCC module containing the different electronic components of the transceiver. The beam steering is achieved using RF-MEMS phase shifters made out of silicon, and integrated in a hybrid fashion onto the ceramic antenna substrate. This work has been motivated by the will to learn about the gain that modern technologies and processes like LTCC and RF-MEMS could bring for the next generation of millimetre wave phased array antennas, where higher integration density, lower fabrication costs and better efficiency is expected.

II. Design of the Antenna Array

The antenna is a four-by-four microstrip antenna array. The antenna array is designed with four sub-arrays connected in parallel by a 1-to-4 corporate feed network. The feed network distributes the RF-power to four feeding microstrip lines. Also, each one of these microstrip lines is used to feed one of the four sub-arrays. The radiating patches are realised on top of the top LTCC layer. The feed network, corporate feed network plus feeding microstrip lines, is processed five layers below the patches, i.e. one LTCC layer above the back-side of the antenna. Three LTCC layers below the patches, a metal plane serving as ground plane for both, the patches and the buried microstrip feed network, is realised. Each one of the four sub-arrays is designed with four patches connected in series by one of the four buried feeding microstrip lines. The patches are connected to their respective feeding line according to the aperture coupling principle. The apertures implemented are H-shaped coupling slots patterned in the common ground plane. A cross-section of the multi-layer ceramic substrate indicating the different features is given in Fig. 1.

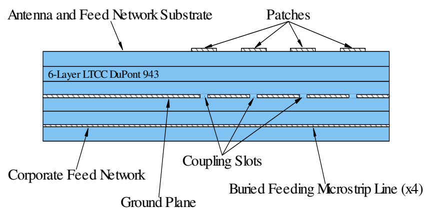

Fig. 1 Cross-sectional view of the fixed beam antenna array on 6-layer LTCC DuPont 943 substrate (the view is not to scale).

The last patch at the end of a sub-array is placed one-quarter of wavelength away from the open-circuited end of the buried feeding microstrip line. This allows for a maximum of magnetic field at the centre of the coupling slot. Since the radiation pattern to achieve in the E-plane is broadside, all four patches of a sub-array have to be fed in-phase. This is done by placing them one guided wavelength away from each others. The coupling slots are centred on the axis of symmetry of the feeding microstrip lines, which have themselves, the same axis of symmetry as the microstrip antennas. In order to minimise the side lobe level of the pattern radiated in the E-plane, an aperture distribution is implemented among the four patches of the sub-arrays by choosing the appropriate length for the different coupling slots. A large coupling slot results in a strong coupling between the feeding line and the radiator and thus, in a large value of the radiating resistance. In return, a small coupling slot corresponds to a weak coupling between the feeding line and the radiator, and it results in a modest radiating resistance. Hence, the sub-arrays of the antenna are designed with 600µm-long coupling slots for the two patches close to the centre of the sub-array, and with 525µm-long coupling slots for the first and last patches. All coupling slots are 100µm-wide. The corporate feed network is designed using asymmetrical T-junction power dividers. They allow for the implementation of an aperture distribution in the H-plane of the aperture. The coefficients used to feed the four sub-arrays have been calculated using the method proposed in [5]. In order to prevent a possible de-lamination of the ceramic tape off the Au-paste used to processed the ground plane, metal-free areas have been patterned in that ground plane. These metal-free areas allow for ceramic-to-ceramic contact regions. They are placed 800µm (approx. $\lambda_d/4$) away from the radiating patches, where the electromagnetic field is negligible. In this way, they do not influence the RF-behaviour of the antenna.

The fixed beam antenna has been measured in anechoic chamber at the University of Ulm. The E- and H-plane far field radiation characteristics are plotted in Fig. 2 and 3, respectively. The measured and simulated return loss of the antenna is plotted in Fig. 4.

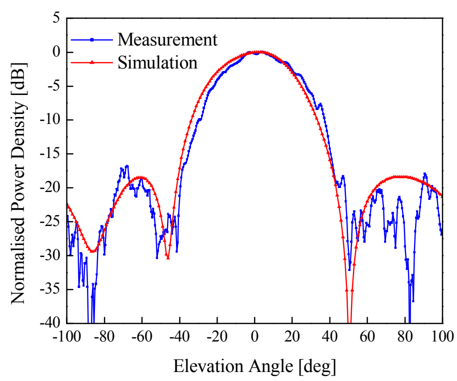

Fig. 2 Measured and simulated E-plane far field pattern of the fixed beam antenna.

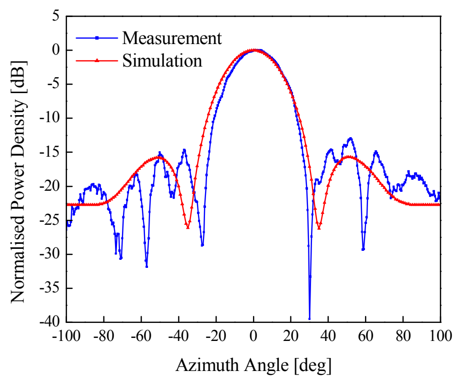

Fig. 3 Measured and simulated H-plane far field pattern of the fixed beam antenna.

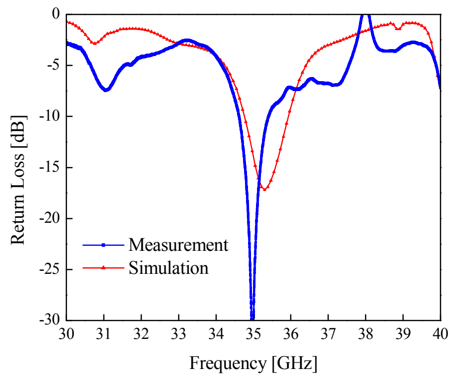

Fig. 4 Measured and simulated return loss of the fixed beam antenna.

Fig. 2, 3, and 4 show good agreement between measurements and simulations. The -3dB beamwidth is 26° and 37° in the H- and E-planes, respectively. The side lobe level is -13dB in the H-plane, and -16.8dB in the E-plane. In the H-plane, the antenna is strictly symmetric and the slight 3° off-axis angle observed between simulation and measurement is believed to be due to an inaccuracy in the positioning of the antenna. This inaccuracy is similar to the one observed in the E-plane (4.5°). The gain of the antenna has been measured at 13.4dB, and the radiation efficiency of the antenna calculated from this value is 65%.

III. Design and Hybrid Integration of the RF-MEMS Phase Shifters

The fixed beam antenna has been equipped with RF-MEMS phase shifters to form a one-dimensional electrically steerable antenna. In order to achieve a beam steering in the H-plane of the aperture, four phase shifters are placed between the corporate feed network and the four antenna sub-arrays. The RF-MEMS phase shifters are processed on silicon dielectric in the EADS Innovation Works technology [6]. They are realised in microstrip technology, and they are processed on 200µm-thick silicon wafers. The four phase shifters are placed in a unique cavity manufactured in LTCC (Fig. 5).

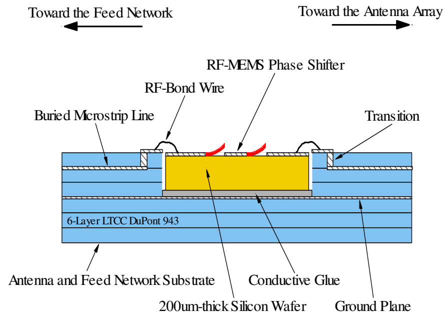

Fig. 5 Hybrid integration of the RF-MEMS phase shifters.

The cavity is fully metallised on the bottom side by a prolongation of the ground plane of the buried microstrip feed network. In order to connect this ground plane to the ground plane of the microstrip phase shifters processed on the back-side of the silicon chips, the phase shifters are fixed in the cavity using conductive glue. The input and output microstrip lines of the phase shifters are connected to the corporate feed network on one side, and to the feeding lines of the antenna sub-arrays on the other side, with Al RF-bond wires. These bond wires are kept as small as possible by minimising the difference in height between the top of the LTCC board and the top of the silicon chips. This is done by manufacturing the cavity with a three-LTCC-layer depth. This 330µm depth corresponds approximately to the height of the silicon chips, once they are placed on about 100µm of conductive epoxy glue. Since the feed network of the antenna is realised with microstrip lines buried one layer above the bottom of the LTCC substrate, they cannot receive directly the RF-bond wires, and a transition has to be implemented. A buried microstrip line to microstrip line transition has been designed using one via to bring the signal line to the top of the LTCC board. A 3D view of this transition is shown in Fig. 6.

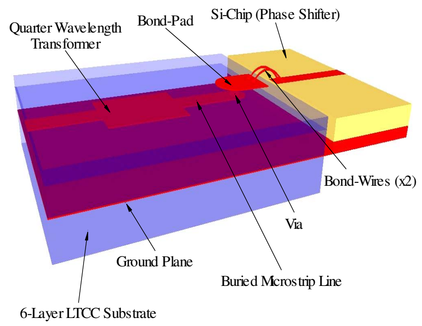

Fig. 6 3D view of the microstrip line transition in LTCC DuPont 943.

The simulated return loss of the transition is below -10dB between 32.25GHz and 37.55GHz. The DC-control lines (not represented in Fig. 5 for a better visibility) necessary to actuate the RF-MEMS switches of the phase shifters are realised in free layers of the LTCC substrate, one and two layers below the ground plane. They are connected to the phase shifters using vias leading to the bottom of the LTCC board, and on top of which bond pads are realised. The bond pads on the LTCC board and the DC-control pads on the silicon chips are connected using DC-bond wires.

IV. Realisation and Measurement of the Electrically Steerable Antenna

A photograph of the complete electrically steerable antenna is shown in Fig. 7.

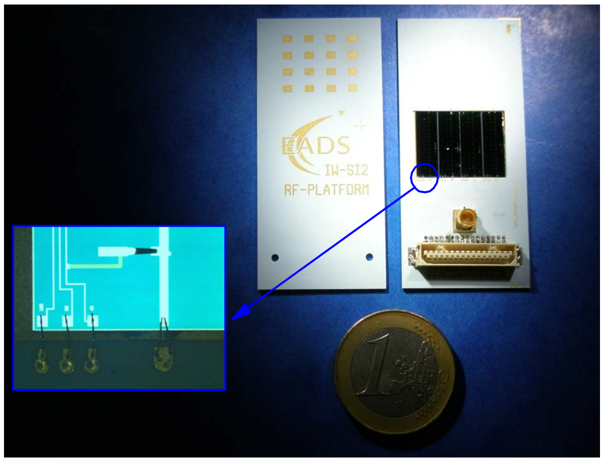

Fig. 7 Photograph of the Ka-band RF-MEMS based electrically steerable antenna on LTCC: front-side (middle), back-side (right) and bond wire connections (left).

The photograph shows the front side as well as the back side of the entire phased antenna. The radiating patches realised on top of the top ceramic layer are visible on the top part of the front-view, depicted in the centre of the photograph. The four phase shifters integrated in a cavity, between the corporate feed network and the sub-arrays can be seen on the back-view of the antenna, on the right-hand side of the picture. Finally, the left-hand part of the figure shows a micrograph of the interface between the phase shifters on silicon and the feed network processed in ceramic. It shows the Al bond wires implemented for both the RF- and the DC-control signals. As shown on the micrograph, two bond wires are used to connect the RF-microstrip line on silicon to the bond pad on ceramic. This aims at reducing the value of the inductance added in series by the bond wires.

The antenna has been characterised in anechoic chamber at the University of Ulm in the same way as the fixed beam antenna. The far field has been measured for three switching states of the phase shifters corresponding to the broadside (0°), and the ±15° steered directions. The measured H-plane far field patterns of the complete phased antenna demonstrator are plotted in Fig. 8.

The measured beams point in the -11°, 4.5°, and in the 22° directions, and have 24°, 21.5°, and 20.2° half-power beam widths, respectively. The side lobe levels are -11.8dB, -8.4dB, and -5dB, respectively.

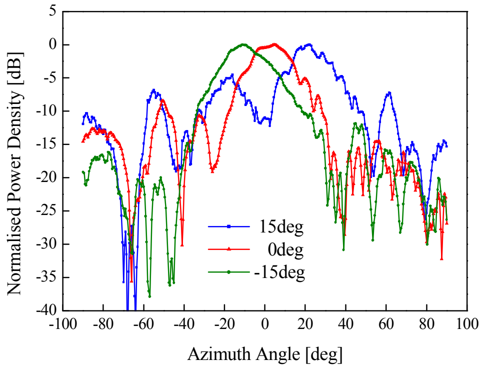

Fig. 8 Measured H-plane steered beams of the RF-MEMS electrically steerable antenna on LTCC.

The partly elevated side lobe level and the inaccuracy of the pointing direction (about 4°) of the three beams could be caused by an inaccuracy in the integration of the silicon chips, e. g. a difference in the length of the bond wires. The return loss of the complete phased array antenna has been measured for both, the broadside and the 15° steered beam cases. The corresponding S_{11}-parameters are plotted in Fig. 9.

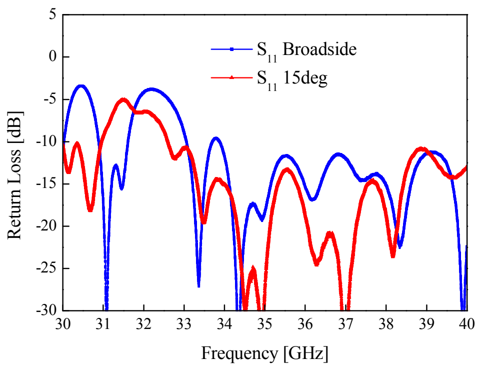

Fig. 9 Measured return loss of the RF-MEMS electrically steerable antenna.

For the pattern pointing in the broadside direction, the measured return loss is below -10dB from 33.88GHz up to above 40GHz. For a beam steered in the 15° direction, it is below -10dB from 32.60GHz up to 40GHz and beyond. The gain of the antenna has been measured for the different pointing directions. It has a satisfactory value of about 8dB for both, the broadside and the -15° patterns. This corresponds to a radiation efficiency of 15.5% for the broadside pattern, and 17.3% for the pattern steered in the -15° direction. The gain of the electrically steerable antenna is 5.4dB below the gain of the fixed beam antenna. This lower gain is explained partly by the insertion loss of the RF-MEMS phase shifters measured at about 2.5dB. The remaining 2.9dB of insertion loss are attributed to the power dissipated in the two transitions between the buried feed network and the bond pads, and in the bond wires.

V. Conclusions

In this paper, a RF-MEMS electrically steerable antenna for communication at Ka-band is demonstrated. The design of the microstrip antenna array on 6-layer LTCC DuPont 943 is described, and the hybrid integration of the RF-MEMS phase shifters is presented. The far field radiation characteristic and the return loss of the proposed phased antenna array are measured for both, the broadside and the ±15° steered directions. The radiation characteristics have beams pointing in the -11°, 4.5°, and 22° directions of the H-plane, and an antenna gain of 8dB is measured for both, the broadside and the steered patterns. The work presented in this exposé constitutes the first steps of a longer development aiming at compact, low-loss, and cost effective phased array antennas for spaceborne communication.

Acknowledgment

This work was supported by the European Commission within the 6th framework program, in the frame of the project RF-Platform (IST-2005-027468).

The authors would like to thank Mr. Peter Feil of the University of Ulm for his helpful assistance, whilst measuring the different far field patterns at Ka-band.

References

[1] S. H. Yisheng and K. Arichandran, “Compact phased array for small leo satellite,” *International Symposium on Antennas, Propagation and EM Theory*, pp 684–687, 2000.

[2] M. Lisi, “Phased arrays for satellite communications: a system engineering approach,” IEEE International Conference on Phased Array Systems and Technology, pp 193–196, 2000.

[3] Y. Zheng and Y. Ruliang, “Feasibility study of using small satellite synthetic aperture radar for global 3D imaging,” *International Geoscience and Remote Sensing Symposium*, volume 6, pp 3162–3164, June 2002.

[4] A. Wicks, A. da Silva-Curiel, J. Ward, and M. Fouquet, “Advancing small satellite earth observation: operational spacecraft, planned missions and future concepts,” *14th AIAA/USU Small Satellite Conference*, August 2000.

[5] W. Gautier, “Array antenna pattern synthesis,” Master Thesis, Ecole Nationale d’Ingénieurs de Brest, September 2005.

[6] C. Siegel, V. Ziegler, B. Schoenlinner, U. Prechtel, and H. Schumacher, “Simplified RF-MEMS switches using implanted conductors and thermal oxide,” *Proceedings of the 36th European Microwave Conference*, September 2006.